CONF-940922--4

Projectile Image Acceleration, Neutralization and Electron Emission during Grazing Interactions of Multicharged Ions with Au(110)

F.W. Meyer, L. Folkerts

Oak Ridge National Laboratory, Oak Ridge, Tennessee 37831-6372

H.O. Folkerts

Kernfysisch Versneller Institut, Zernikelan 25, NL 9747 AA Groningen, The Netherlands

S. Schippers*

Oak Ridge National Laboratory, Oak Ridge, Tennessee, 37831-6372
and Osnabrück University, D-49069 Osnabrück, Germany

Abstract

Recent Oak Ridge work is summarized on projectile energy gain by image charge acceleration, scattered ion charge distributions, and K-Auger electron emission during low energy grazing interactions of highly charged Pb, I, O and Ar ions with a Au(110) surface.

Introduction

In this contribution we present results of recent Oak Ridge work in the area of low energy multicharged ion-surface interactions. In the first section measurements of angular distributions of multicharged Pb and I projectiles scattered from Au(110) under grazing incidence conditions are discussed. Measurements of projectile angular scattering distributions are of interest in the present context because they permit determination of projectile energy gains due to image charge acceleration on the approach trajectory. These energy gains directly reflect the evolution of the effective projectile charge as a function of above-surface distance, and thus provide a convenient window on the study of above-surface neutralization processes relevant

MASTER

DISTRIBUTION OF THIS DOCUMENT IS UNLIMITED

DISCLAIMER

Portions of this document may be illegible in electronic image products. Images are produced from the best available original document.

to multicharged ion-surface interactions. In the second section recent measurements of scattered projectile charge state distributions for multicharged O projectiles are discussed, with emphasis on their utility in determining capture rates. In the final section, we turn to a related aspect of multicharged ion-surface interactions, namely K-Auger electron emission, and present a modelling study of the K-Auger lineshape for Ar^{17+} incident on Au(110) at 20°. For this last incidence condition, sub-surface K-Auger electron emission is the dominant contributor to the observed projectile K-Auger spectrum. The goal of this simulation was to obtain additional insight into sub-surface neutralization processes via the determination of the L-shell population at the time of the K-Auger emission. The simulation incorporates a simple neutralization model for obtaining the depth distribution of the sub-surface K-Auger emission, L-shell population dependent state-to-state K-Auger transition energies calculated using the Cowan code, as well as Doppler broadening and electron transport effects on the observed lineshape.

Image Acceleration Energy Gain Measurements

Using the recently developed metal ion production capability of the new ECR source recently brought on-line in the ORNL Multicharged Ion Research Facility, together with a recently installed 2-D position sensitive detector, we have made measurements of angular scattering distributions for 150 - 300 keV Pb^{q+} ($11 \leq q \leq 36$) and I^{q+} ($10 \leq q \leq 25$) ions grazingly incident on Au(110). The motivation behind the measurements was to determine the perpendicular projectile energy gain due to image charge acceleration prior to surface impact, over a range of charge states overlapping earlier measurements by Winter et al.[1] using Xe^{q+} ions, also made under grazing incidence conditions. These earlier measurements showed some evidence of a deviation from the $q^{3/2}$ charge state dependence[1,2] expected under the assumption of step-wise over-the-barrier neutralization above the surface.

The experimental procedure is briefly described as follows. After collimation of the incident Pb or I multicharged ion beams by two 0.5-mm-diameter apertures to an angular divergence of about 0.1° FWHM, the ions are incident on a clean Au (110)

target at ~1° along the (100) direction. The scattering geometry is indicated schematically in Fig. 1. The single crystal Au(110) target is mounted on an x-y-z manipulator located in a UHV chamber having a base pressure of $3x10^{-10}$ mbar and is prepared by cycles of surface sputter cleaning with 1-keV Ar^+ ions and crystal annealing at about 700°C. Surface cleanliness is verified using electron-induced Auger electron spectroscopy. Both the angular distribution (polar as well as lateral) and charge state distribution of the scattered (reflected) projectiles could be measured using a two-dimensional position sensitive detector (PSD) (Quantar Technology Model 3394A) having a 40-mm-diameter active area. Movable slits located between the target and the PSD were completely opened for measurements of angular scattering distributions. For the charge state distribution measurements they were closed to select a thin vertical slice of the scattered beam, which was then dispersed by charge state across the face of the PSD using a pair of electrostatic deflection plates located immediately downstream of the slit assembly, as shown in Fig. 1. The target-PSD distance is about 560 mm. The PSD is mounted on a second x-y-z manipulator which permits measurement of the polar scattering angle, ϕ_p, in the range -0.8° to +5.6°. The position of the primary beam, used to determine $\phi_p = 0°$, as well as its angular spread, can thus be directly measured.

The above-surface projectile energy gains were inferred from the observed projectile reflection angles in a manner described elsewhere[1,3,4]. The incidence angle was determined by measuring the total scattering angle for a low charge state ion beam such as O^+ where image acceleration effects are minimal. The effect of small stray magnetic fields on the actual target incidence angle was corrected for by using the small (but measurable) position shifts of the various primary charge state beams on the PSD to deduce the slight, charge-dependent projectile trajectory curvature at the target position, as discussed in greater detail in Ref. 4. Charge analysis performed on the scattered ions showed that neutrals were the dominant charge state by far, as has also been observed by others[1,3,5], indicating that the observed image acceleration effects occured on the incident (approach) trajectory.

Fig. 2 shows the experimentally deduced projectile energy gains as a function

of incident charge state. As can be seen from the figure, for charge states up to +29, the inferred energy gains were found to have the expected q dependence. Furthermore, in the region of charge state overlap, the energy gains inferred for the I^{q+} and Pb^{q+} were, within the experimental uncertainty, the same. For charge states 30+ and higher, however, the determined energy gains are seen to fall systematically below the expected $q^{3/2}$ trend, just as has been observed by Winter et al.[1] In view of the different ionic species used in the present experiment, this effect is not likely to result from the projectile atomic structure. Energy gains inferred from studies of the saturation of potential emission induced by normally incident ions of charge state up to +72 show no evidence[6] of such a deviation, and suggest that the presence of the relatively large parallel velocity components in the case of the grazing geometry measurements may have more significant implications for the above-surface neutralization of multicharged ions than previously thought.

Scattered Projectile Charge State Distribution Measurements

As mentioned in the previous section, in order to determine the charge distribution of the scattered ions, movable slits were used to select a vertical slice of the scattered beam, which then passes through a set of deflection plates. The electrostatic analysis produces a series of horizontally displaced vertical bands, each corresponding to a particular charge state, while the intensity distribution of each band along the vertical axis reflects its polar angular distribution. The charge state distributions can be obtained by collapsing the 2D spectrum onto the horizontal axis. Integration under each charge state "peak" then permits determination of the scattered charge state fractions[7]. This was done for oxygen ions in initial charge states down to q=3, and for Ar ions in the incident charge state range 3-14. Results are given for 3.75 keV/amu O^{q+} ions incident on Au(110) along the [110] direction at 1.8° in Fig. 3, where the fractions of final charge states "r" are plotted as a function of the incident charge state "q". For this case, the movable slits were set to select lateral angles ϕ_i from -0.15° to +0.15°, i.e. a central slice from the scattered ion angular distribution.

A number of remarkable features can be noted in this figure. For all incident charge states investigated, the neutral fraction strongly dominates the scattered ion charge state distribution, as has been also been noted in connecton with the energy gain measurements described in the previous section. For incident ions not carrying inner shell vacancies, i.e. $q \leq 6$, the scattered charge fractions are essentially independent of incident charge, indicating complete charge equilibration. A significant fraction of the scattered ions recede from the surface in charge state -1, as has also been observed by others[5,9]. As can be seen from the figure, the scattered ion fractions of charge state +2 and higher, while constituting less than 1% of the total scattered ion flux, show noticeable increases when the incident ion carries initial K-shell vacancies, i.e. for O^{7+} and O^{8+}. Such a trend has been previously noted by de Zwart et al.[9]

We attribute this increase to a very small fraction of K-vacancies that have survived the interaction with the surface, and which instead decay sufficiently far above the surface that reneutralization cannot occur. This is illustrated in Fig. 4, which shows a simulation of the charge state evolution during interaction with the surface for three different incident oxygen charge states: O^{6+}, O^{7+} , and O^{8+}. The simulation considers the competition between step-wise filling and depletion of the L-shell at empirically determined[10] rates of 10^{15} s^{-1} and 10^{14} s^{-1} , respectively (the latter is increased to 10^{16} s^{-1} for the case of the O^{-} charge fraction), which, as can be seen from the top panel of the figure, achieves an equilibration of charge states after about 20 fs, in a distribution that agrees roughly with experiment. When the K-shell is opened, the introduction of K-Auger decay at an L-shell population-dependent rate, determined using the Cowan Hartree Fock code[11] (see Fig. 4 for functional form used), gives a set of charge fractions <u>with</u> surviving K-vacancies that decay roughly exponentially for interaction times greater than 15-20 fs. The charge fractions <u>with</u> K-vacancy that survive the 25 fs surface interaction time (as deduced by projectile trajectory calculations[10]) will undergo K-Auger decay without reneutralization and will thus contribute to the next higher charge state seen at infinity. Thus the fraction labelled "+0 with K-vac" in the second panel of Fig. 4 will contribute about 5% to the

+1 asymptotic charge state assuming an interaction time of 25 fs. Introduction of a second initial K-vacancy (see bottom panel of figure for decay rate) further delays complete relaxation or equilibration, and in effect roughly doubles the contribution to the asymptotic +1 charge fraction by K-Auger decay on the receeding projectile trajectory. It is noted that with the rates quoted above, even with two K-vacancies, essentially complete charge equilibration has been achieved after 25 fs, in accord with the observation (Fig. 3).

Projectile K-Auger lineshape simulation studies

Installation of the new CAPRICE ECR ion source has permitted measurement[12] of projectile K-Auger electron emission during interaction of Ar^{17+} and Ar^{18+} ions with Au(110). In an attempt to obtain information from the observed K-Auger lineshape on sub-surface neutralization, a lineshape simulation is under development to deduce the L-shell population of the Ar projectile at the time of the K-Auger decay. Preliminary results are presented below for the incident Ar^{17+} case. Since the simulation is discussed in greater detail elsewhere[13], only its main features are briefly summarized here. The simulation assumes isotropic K-Auger electron emission in the frame of the projectile moving along a straight line trajectory determined by the asymptotic incidence angle. Doppler broadening effects were included by proper transformation of the electron energy to the laboratory frame. While the depth distribution of the K-Auger emission can be determined via a neutralization model such as has been described in the previous section, the present preliminary results were obtained by assuming an infinitely fast L-shell filling starting at 2Å above the surface, followed by the K-Auger transition itself with the published[14] rate of 7.5×10^{14} s^{-1}, i.e. the simplest possible one-step model.

Transport of those electrons emitted below or toward the surface was treated using a Monte Carlo simulation[15] in which both elastic and inelastic scattering was incorporated, as has been discussed also by Bleck-Neuhaus et al.[16]. In order to avoid multiple length scales in the Monte Carlo simulation, the inelastic scattering

contribution to the simulated lineshape is obtained by calculating the electron energy loss (using the known stopping power of electrons in Au[17]) for those electrons who do not escape the bulk prior to their first inelastic encounter. The simulated K-Auger lineshape was obtained by convoluting the calculated lineshape for a single electron energy (i.e. delta function source term) with the manifold of possible transition energies for a given initial L-shell population, whose relative weighting was determined by the total angular momentum J of the different initial states. The transition energies were calculated using the Cowan Hartree Fock code[11] implemented via a UNIX shell developed by Schippers[18]. Best agreement with the experimentally observed KLL-Auger spectrum is obtained by including only those transitions originating from a filled L-shell, i.e. from the initial configuration $1s^1\ 2s^2\ 2p^6\ 3s^2\ 3p^6$. A similar procedure was used for the KLM transitions. It was found that the transitions from the initial configuration $1s^1\ 2s^2\ 2p^2\ 3s^2\ 3p^6\ 3d^4$ gave a simulated lineshape that agreed best with experiment. Fig. 5 shows the resulting composite simulated K-Auger spectrum together with the experimentally observed spectrum. The intensity ratio of KLL and KLM contributions in the simulation that gave the best fit to the measured spectrum was 1/0.35. It is noted that the state of L-shell filling deduced from the KLL and KLM peaks appear to be inconsistent. However, in the case of the KLM peak simulation, unlike that for the KLL peak, the transition energies were found to depend quite sensitively on the assumed M-shell population. Since the M-shell is most likely immersed in the metal valence band, it is not obvious what the appropriate M-shell population and the extent of bulk screening effects on the relevant M-shell binding energies might be. For this reason, among others, we feel that the conclusions drawn from this preliminary KLM fit are subject to more uncertainty than those based on the KLL analysis.

Acknowledgements

This research was sponsored by the Division of Applied Plasma Physics, Office of Fusion Energy, and by the Division of Chemical Sciences, Office of Basic Energy Sciences of the U.S. Department of Energy under contract No. DE-AC05-84OR21400

with Martin Marietta Energy Systems, Inc. L. Folkerts was supported through a program administered by the Oak Ridge Institute for Science and Education. S. Schippers gratefully acknowledges financial support by the Deutsche Forschungsgemeinschaft (DFG).

*Present address: Kernfysisch Versneller Instituut, Zernikelaan 25, 9747 AA Grongingen, The Netherlands,

References

[1]H. Winter, C. Auth, R. Schuch, and E. Beebe, Phys. Rev. Lett 71, 1939 (1993).

[2]J. Burgdörfer and F.W. Meyer, Phys. Rev. A 47, R20 (1993).

[3]H. Winter, Europhys. Lett 18, 207 (1992).

[4]L. Folkerts, H. O. Folkerts, and F.W. Meyer, to be submitted to Phys. Rev. A.

[5]M. A. Briere, D. Schneider, J. McDonald, M. Reeves, C. Rühlicke, G. Weinberg, and D. Knapp, NIM B90, 231 (1993); M.A. Briere, D. Schneider, T. Schenkel, C. Rühlicke, and M. Reeves, this conference proceedings.

[6]F. Aumayr, H, Kurz, D. Schneider, M.A. Briere, J.W. McDonald, C.E. Cunningham, and HP. Winter, Phys. Rev. Lett. 71, 1943 (1993).

[7]F.W. Meyer, L. Folkerts, and S. Schippers, Proceedings of the 10th International Workshop on Ion Solid Collisions, Grand Targhee, Wy, Aug. 8-12, 1994, to be published in NIMB.

[8]I.H. Hughes, S. Hustedt, J. Limburg, N. Hatke, R. Hoekstra, W. Heiland, and R. Morgenstern, this conference proceedings.

[9]S.T. de Zwart, T. Fried, U. Jellen, A.L. Boers, and A.G. Drentje, J. Phys. B18, L623 (1985).

[10]L. Folkerts, S. Schippers, D.M. Zehner, and F.W. Meyer, submitted to Phys. Rev. Lett.

[11]R.D. Cowan, *The Theory of Atomic Structure and Spectra*, (California University Press, Berkeley, 1981).

[12]L. Folkerts and F.W. Meyer, Abstracts of Contributed Papers of the XVIII ICPEAC,

Aarhus, Denmark, 21-27 July, 1993, ed. T. Anderson, B. Fastrup, F. Folkmann, and H. Knudsen, p. 770.

[13]L. Folkerts and F.W. Meyer, to be submitted to Phys. Rev. A.

[14]e.g. C.P. Bhalla, Phys. Rev. A8, 2877 (1973).

[15]Based on Monte Carlo routines developed by David C. Joy, University of Tennessee and Oak Ridge National Laboratory; e.g. David C. Joy, J. Microscopy 147, 51 (1987).

[16]J. Bleck-Neuhaus, A. Saal, R. Page, P. Biermann, R. Köhrbrück, and N. Stolterfoht, Phys. Rev. A49, R1539 (1994); J. Bleck-Neuhaus, R. Page, and A. Saal, NIMB 78, 113 (1993).

[17]J.C. Ashley, J. Elect. Spect. Rel. Phen. 50, 323 (1990).

[18]S. Schippers, KVI Internal Report KVI-189i, Groningen, The Netherlands, 1994.

Figure Captions

Fig. 1. Schematic side and top views of the collision geometry and experimental layout.

Fig. 2. Projectile energy gain by image charge acceleration for 150 keV I^{q+} and Pb^{q+} ions incident at ~1° on Au(110), as a function of projectile charge state.

Fig. 3. Scattered projectile charge fractions for 3.75 keV/amu O^{q+} ($3 \leq q \leq 8$) ions incident at 1.8° along the [110] direction of Au(110).

Fig. 4. Simulated charge fraction evolution with interaction time for O^{6+} (top panel), O^{7+} (middle panel), and O^{8+} (bottom panel) incident ions. The relevant single capture and loss rates, as well as K-Auger decay rates used are indicated to the right of the panels.

Fig. 5. Comparison of simulated and measured projectile K-Auger electron spectra for Ar^{17+} incident on Au(110) at 20°. Both spectra correspond to observation at 90° to the incident beam direction.

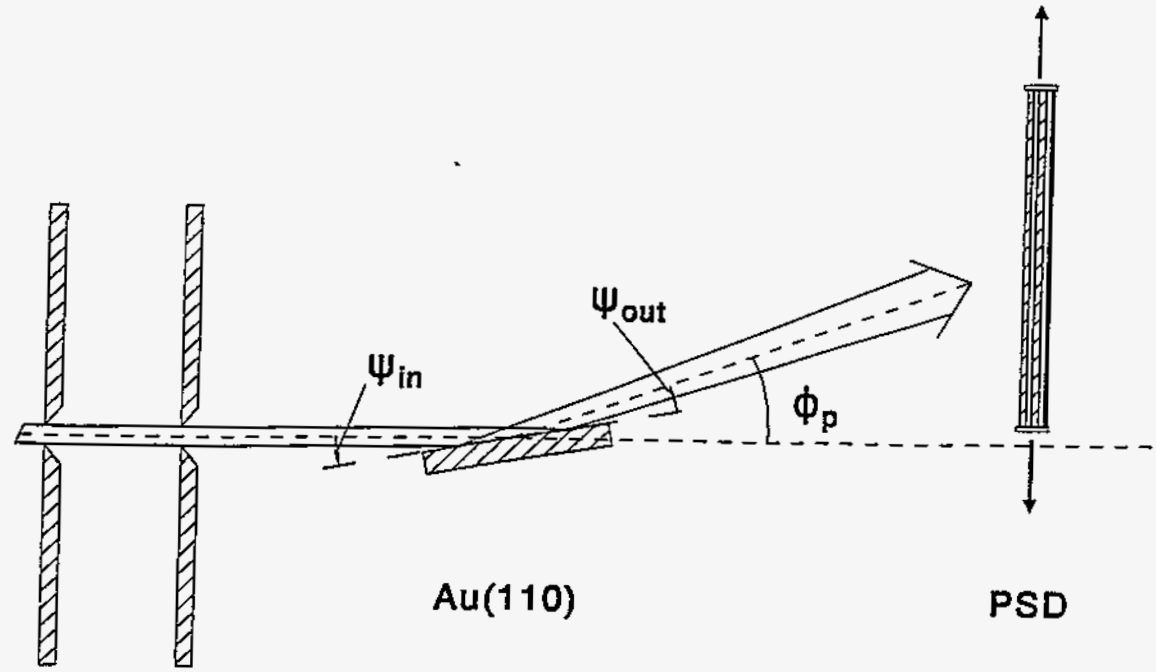

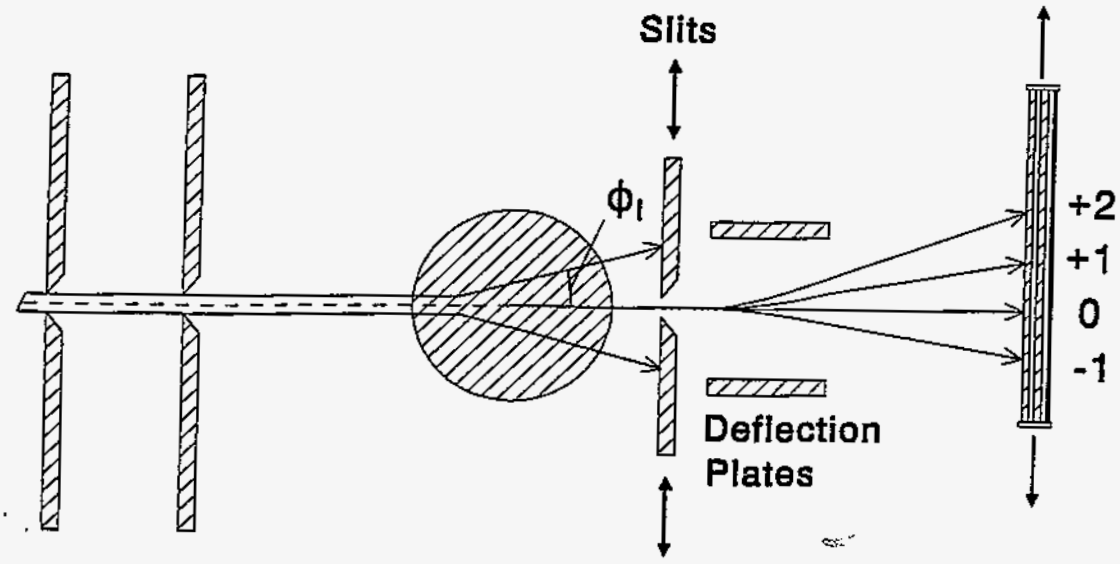

DISCLAIMER

This report was prepared as an account of work sponsored by an agency of the United States Government. Neither the United States Government nor any agency thereof, nor any of their employees, makes any warranty, express or implied, or assumes any legal liability or responsibility for the accuracy, completeness, or usefulness of any information, apparatus, product, or process disclosed, or represents that its use would not infringe privately owned rights. Reference herein to any specific commercial product, process, or service by trade name, trademark, manufacturer, or otherwise does not necessarily constitute or imply its endorsement, recommendation, or favoring by the United States Government or any agency thereof. The views and opinions of authors expressed herein do not necessarily state or reflect those of the United States Government or any agency thereof.

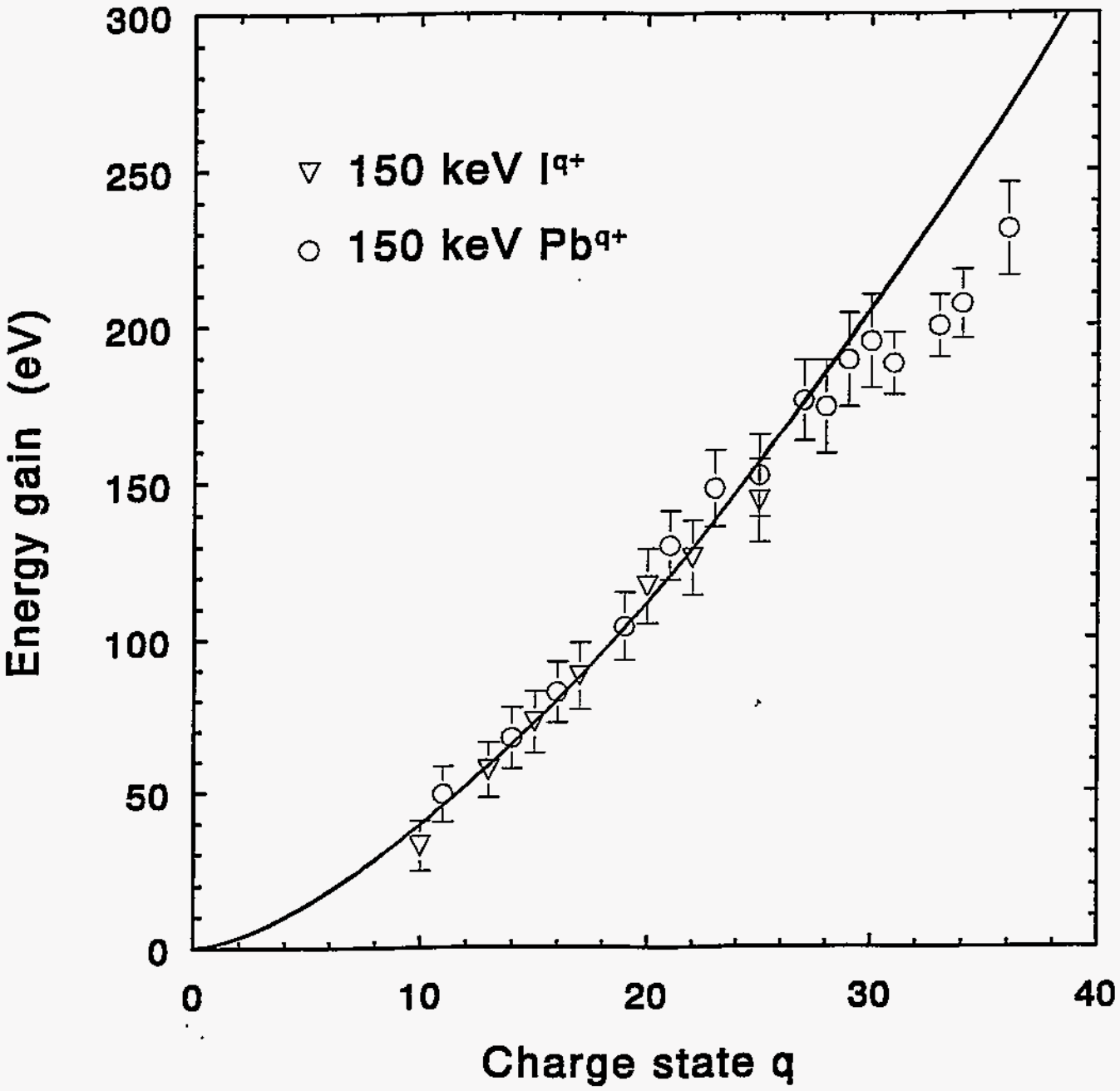
300
250
200
150
100
50
0
Energy gain (eV)
150 keV I^q+
150 keV Pb^q+
0
10
20
30
40
Charge state q

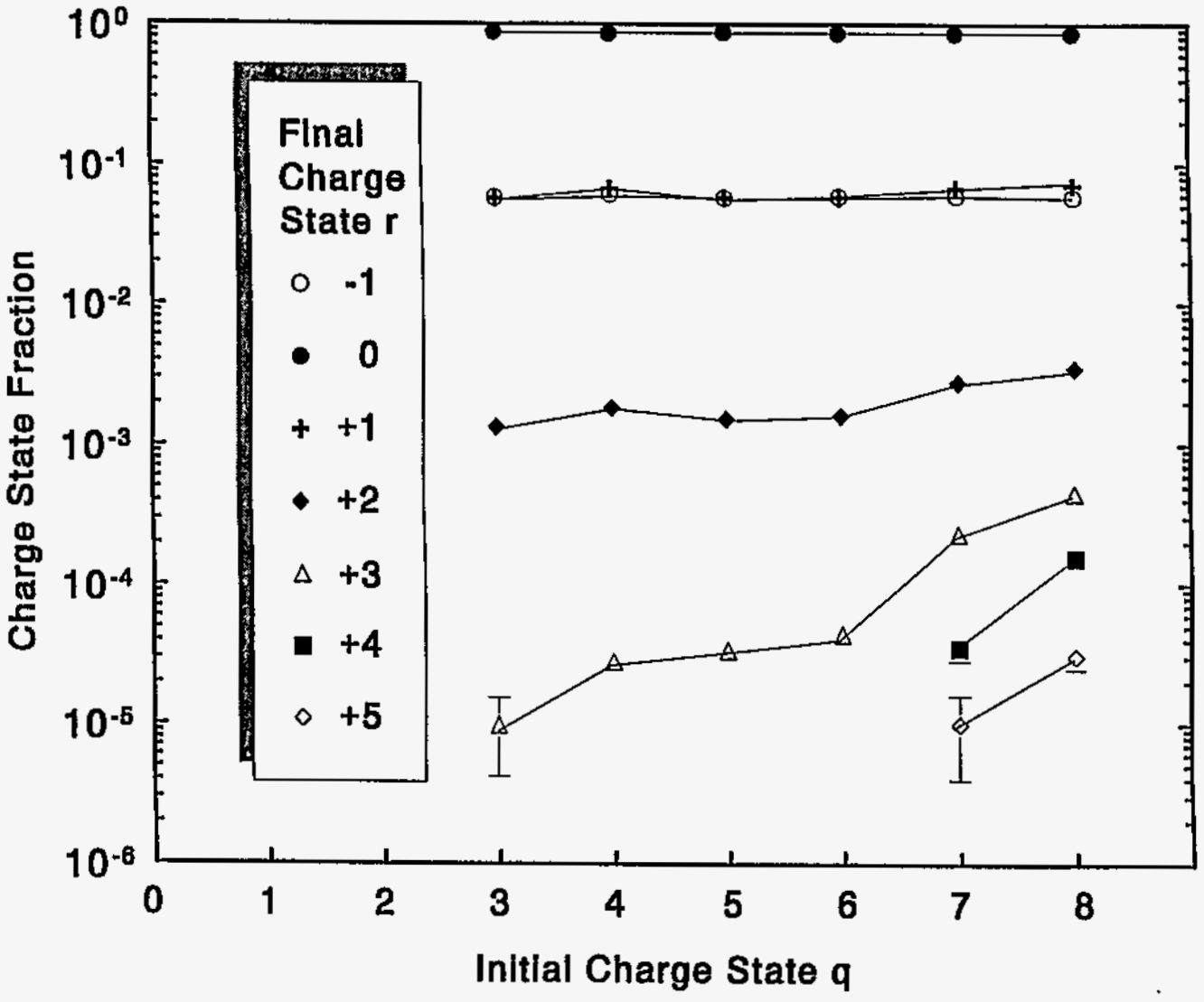
Charge State Fraction
10^{0}
10^{-1}
10^{-2}
10^{-3}
10^{-4}
10^{-5}
10^{-6}
0
1
2
3
4
5
6
7
8
Initial Charge State q
Final Charge State r
-1
0
+1
+2
+3
+4
+5

Fig 3

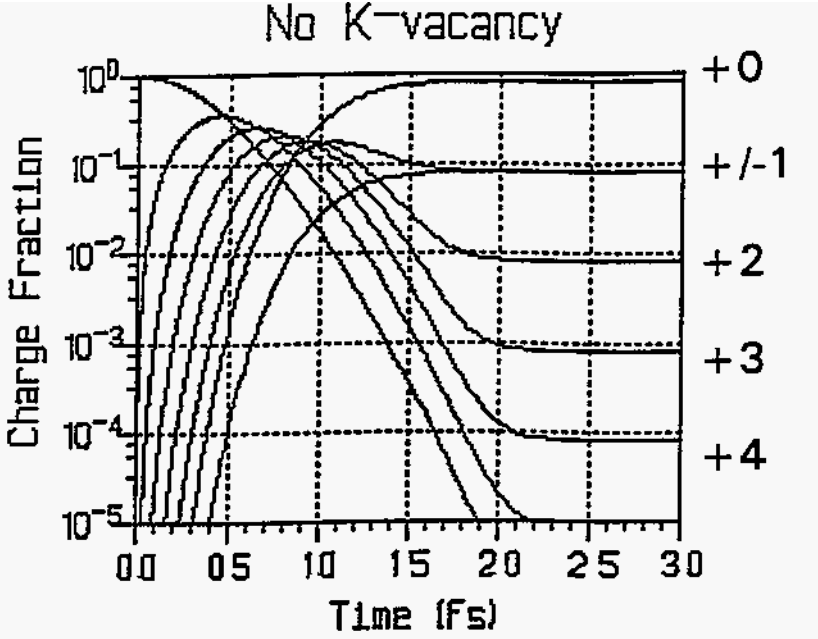

1-Electron capture rate:

$1 \times 10^{15}\ s^{-1}$

Ionization rate:

$10 \times 10^{15}\ s^{-1}$

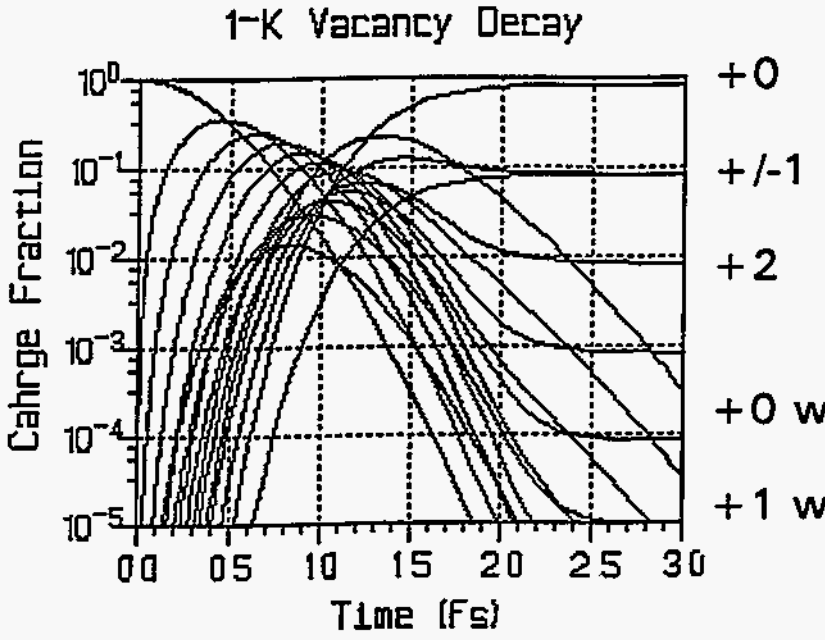

Single K-vacancy K-Auger rate:

$0.29 * n_L * 10^{14}\ s^{-1}$

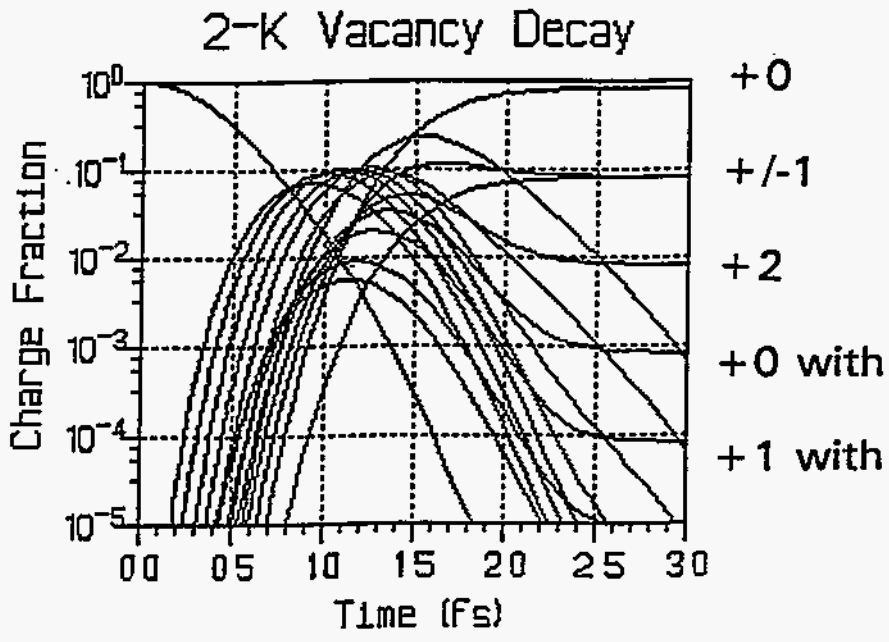

Double K-vacancy K-Auger rate:

$0.85 * n_L * 10^{14}\ s^{-1}$

283 keV Ar^{17+} incident on Au(110) at 20°